Relaxation-Assisted Separation of Chemical Sites in NMR Spectroscopy of Static Solids

ARTICLE *in* JOURNAL OF THE AMERICAN CHEMICAL SOCIETY · APRIL 2003

Impact Factor: 12.11 · DOI: 10.1021/ja021173m · Source: PubMed

3 AUTHORS, INCLUDING:

Mrignayani Kotecha
University of Illinois at Chicago
25 PUBLICATIONS **404** CITATIONS
SEE PROFILE

Lucio Frydman
Weizmann Institute of Science
220 PUBLICATIONS **6,108** CITATIONS
SEE PROFILE

J|A|C|S
ARTICLES
Published on Web 00/00/0000

Relaxation-Assisted Separation of Chemical Sites in NMR Spectroscopy of Static Solids

Adonis Lupulescu, Mrignayani Kotecha, and Lucio Frydman*

Contribution from the Department of Chemical Physics, Weizmann Institute of Sciences, 76100 Rehovot, Israel

Received September 12, 2002; E-mail: lucio.frydman@weizmann.ac.il

Abstract: We discuss the potential use of relaxation times toward the resolution of inequivalent chemical sites in the NMR spectroscopy of powdered or disordered samples. This proposal is motivated by the significant differences that can often be detected in the relaxation behavior of sites in solids, particularly when focusing on NMR observations of quadrupolar nuclei possessing different coordination and/or dynamic environments. It is shown that in these cases the implementation of a non-negative least-squares analysis on relaxation data sets enables the bidimensional resolution of overlapping powder line shapes, even when dealing with static samples. In combination with signal-enhancement methodologies such as the quadrupolar Carr−Purcell Meiboom−Gill train, such relaxation-assisted separations open up valuable routes toward the high-resolution characterization of systems involving insensitive (e.g., low-γ) nuclei. The principles and limitations of the 2D NMR approach resulting from these considerations are discussed, and their potential is exemplified with a variety of static and spinning investigations. Their extension to other nuclear systems where spectral resolution is problematic, such as protons in organic solids, is also briefly considered.

Introduction

A distinctive challenge of nuclear magnetic resonance (NMR) experiments on solid samples is the achievement of spectral resolution. Whereas liquid-phase molecules undergoing fast isotropic tumbling lead to sharp and well-resolved NMR peaks, sites from solids yield broad resonances that usually overlap with one another.[1,2] This line broadening originates from the anisotropy of the nuclear spin interactions, and it can impose severe sensitivity and resolution penalties on the spectroscopy. Averaging away the anisotropic parts of the spin interactions has consequently been a topic of continuous investigation in high-resolution solid-state NMR.[1−4] Foremost among the strategies proposed to retrieve narrow peaks from solids is magic-angle-spinning (MAS), a relatively simple mechanical procedure capable of removing all anisotropies that transform as second-rank tensors.[5,6] On the other hand, it is well-known that by itself MAS is unable to average away certain anisotropies, such as the second-order quadrupole line broadening that often arises when considering nuclei with spin ≥ 1.[7−10] These effects dominate the central-transition spectroscopy of half-integer quadrupolar nuclei, where they will often broaden resonances by several kHz. Driven by the need for techniques capable of facilitating the study of these nuclei—and thereby of the numerous technologically important materials in which they participate[11−13]—new techniques were introduced during recent years for improving both the resolution and the sensitivity of quadrupolar NMR. The former include methods such as dynamic-angle spinning, multiple-quantum MAS (MQMAS), and satellite-transition MAS, techniques which can afford liquid-like NMR spectra by incorporating into conventional MAS additional manipulations of the spins' evolution.[14−18] Central among the latter has been the implementation of Carr−Purcell Meiboom−Gill (CPMG) echo trains[19,20] in conjunction with the signal's acquisition, an approach that under suitable conditions can enhance the normal single-pulse sensitivity achievable per unit time by an order of magnitude.[21−23]

* To whom correspondence should be addressed. Fax: +972-8-9344123.

(1) Abragam, A. *Principles of Nuclear Magnetism*; Oxford University Press: New York, 1961.
(2) Ernst, R. R.; Bodenhausen, G.; Wokaun, A. *Principles of Nuclear Magnetic Resonance in One and Two Dimensions*; Clarendon: Oxford, 1987.
(3) Haeberlen, U. In *Advances in Magnetic Resonance, Supplement 1*; Waugh, J. S., Ed.; Academic Press: New York, 1976.
(4) Schmidt-Rohr, K.; Spiess, H. W. *Multidimensional Solid-State NMR and Polymers*; Academic Press: London, 1994.
(5) Andrew, E. R.; Bradbury, A.; Eades, R. G. *Nature* **1958**, *182*, 1659.
(6) Lowe, I. J. *Phys. Rev. Lett.* **1959**, *2*, 285.
(7) Ganapathy, S.; Schramm, S.; Oldfield, E. *J. Chem. Phys.* **1982**, *77*, 4360.
(8) Freude, D.; Haase, J. In *NMR Basic Principles and Progress*; Diehl, P., Fluck, E., Guenther, H., Kosfeld, R., Seelig, J., Eds.; Springer-Verlag: New York, 1993; Vol. 29, p 1.
(9) Smith, M. E.; vanEck, E. R. H. *Prog. NMR Spectrosc.* **1999**, *34*, 159.
(10) Frydman, L. *Annu. Rev. Phys. Chem.* **2001**, *52*, 463.
(11) Maciel, G. E. *Science* **1984**, *226*, 282.
(12) Fitzgerald, J. *Solid State NMR of Inorganic Materials*; Washington, DC, 1999.
(13) Anderson, M. W., Duer, M. J., Eds. New NMR Techniques for Quadrupolar Nuclei. *Solid State NMR*, **1999**, *15*.
(14) Wooten, E. W.; Muller, K. T.; Pines, A. *Acc. Chem. Res.* **1992**, *25*, 209.
(15) Frydman, L.; Harwood: J. S. *J. Am. Chem. Soc.* **1995**, *117*, 5367.
(16) Medek, A.; Harwood: J. S.; Frydman, L. *J. Am. Chem. Soc.* **1995**, *117*, 12779.
(17) Gan, Z. H. *J. Am. Chem. Soc.* **2000**, *122*, 3242.
(18) Gan, Z. H. *J. Chem. Phys* **2001**, *114*, 10845.
(19) Carr, H. Y.; Purcell, E. M. *Phys. Rev.* **1954**, *94*, 630.
(20) Meiboom, S.; Gill, D. *Rev. Sci. Instrum.* **1958**, *29*, 688.
(21) Larsen, F. H.; Jakobsen, H. J.; Ellis, P. D.; Nielsen, N. C. *J. Phys. Chem. A* **1997**, *101*, 8597.
(22) Larsen, F. H.; Skibsted, J.; Jakobsen, H. J.; Nielsen, N. C. *J. Am. Chem. Soc.* **2000**, *122*, 7080.
(23) Lipton, A. S.; Buchko, G. W.; Sears, J. A.; Kennedy, M. A.; Ellis, P. D. *J. Am. Chem. Soc.* **2001**, *123*, 992.

10.1021/ja021173m CCC: $25.00

Though highly significant, these advances in resolution and sensitivity do not yet offer a general, ideal route to the study of half-integer quadrupolar nuclei in solids. The resolution enhancement methods, for instance, applicable as they are to a wide variety of species, are usually associated with losses that make them ill-suited to study systems characterized by poor signal-to-noise ratios (S/N). Quadrupolar CPMG, on the other hand, works best when applied on static systems affected by severe inhomogeneous quadrupolar broadening, a scenario where achieving site resolution is unlikely. In the course of carrying out various experiments on half-integer quadrupolar nuclei, and while looking for ways to alleviate these challenges, our attention was called by a distinctive behavior that we believe offers a valuable alternative to enhancing spectral resolution in either spinning or static solids. This arises from the highly heterogeneous longitudinal relaxation behavior displayed by quadrupolar nuclei, where T_1 values differing by orders of magnitude are often observed between chemically inequivalent sites. This heterogeneity within the crystalline lattice can be traced to the highly local nature of the quadrupolar relaxation process, dependent mostly on the degree of electronic symmetry surrounding a spin and on the dynamics occurring within the nucleus' immediate vicinity. When combined with the conveniently short T_1 values that quadrupole nuclei usually possess in solids, this feature opens up a route for the discrimination of inequivalent sites based on their spin relaxation behavior rather than on their isotropic shifts. The following section describes the numerical and experimental methodologies that were employed to test this relaxation-assisted separation (RAS) of solid-state NMR resonances; subsequent sections illustrate and assess the results achievable by this type of strategy under various conditions.

Numerical and Experimental Methods

Though the systematic use of relaxation time differences has to the best of our knowledge not been employed for enhancing the resolution of solid-state quadrupolar NMR spectra, the separation of structures based on their dynamic behavior is common in many areas of magnetic resonance. The selective contrast according to relaxivity or diffusivity characteristics of otherwise isochronous water signals serves as a routine diagnostic tool in magnetic resonance imaging.[24,25] NMR applications of two-dimensional diffusion-ordered spectroscopy (2D DOSY) have also become common in the discrimination of liquid-state resonances arising from chemical mixtures according to their originating compound.[26−29] Relaxation differences have also been recently exploited to separate ^{13}C CPMAS NMR resonances arising from different polymorphs as well as to probe dynamics within the context of 2D chemical exchange.[30,31] On exploring the potential extension of the principles underlying these techniques to the resolution enhancement of solid-state quadrupolar NMR, an approach similar to that involved in 2D DOSY was adopted. The separation of sites according to their relaxation characteristics begins in the resulting protocol with the collection of a normal set of NMR signals, as a function of a parameter τ encoding the spins' relaxation behavior. Given their additional dependence on the acquisition time t encoding the spins' evolution frequencies, such 2D set of signals can be described as

$$S(\tau,t) = \int\int I(\nu,R)\,\exp[i\nu t]G(R,\tau)\mathrm{d}\nu\mathrm{d}R \qquad (1)$$

$I(\nu,R)$ is a distribution separating the quadrupolar powder line shapes of the different sites that are present in the sample according to their relaxation rates R, and in the present instance constitutes the 2D data set being sought. The τ-encoded G function in eq 1 describes the relaxation process that is followed; i.e., $G(R,\tau) = \exp[-R\tau]$ when measuring an exponential decay or $G(R,\tau) = 1 - \exp[-R\tau]$ when dealing with a saturation-recovery behavior. Inverting eq 1 to extract $I(\nu,R)$ from $S(\tau,t)$ can formally be summarized by a Fourier transform of S against t, which extracts the frequency distributions that are present, followed by an inverse Laplace transform against τ which finds the rates contributing to the spins' relaxation at a particular frequency within the powder pattern:

$$S(t,\tau) \xrightarrow{FT(t)} P(\nu,\tau) \xrightarrow{LT^{-1}(\tau)} I(\nu,R) \qquad (2)$$

Despite the procedure's apparent simplicity, the last inversion constitutes a main challenge in the relaxation-assisted separation of peaks. By contrast to the extraction of frequencies via Fourier analysis, which is a well-behaved operation, the inversion of a real decaying function to extract multiple decay rates is remarkably unstable. Numerous strategies have consequently been proposed to implement a robust numerical inversion of exponential recovery data in terms of their rate components.[26−36] For the purpose of the present exploratory study, we decided to assay what is perhaps the simplest of these strategies, based on a non-negative least-squares (NNLS) fitting of the relaxation data. Such analysis employed as input the purely absorptive powder patterns $P(\nu,\tau)$ measured throughout the recovery series, and modeled the relaxation behavior for each individual frequency ν according to an idealized sum

$$P(\nu,\tau) = \sum_R A_\nu(R)G(R,\tau) \qquad (3)$$

$A_\nu(R)$ describes here the (positive) contribution that each particular rate R makes to the frequency's relaxation, and its determination lies at the core of the NNLS search. To find these preexponential coefficients, a range of potential relaxation rates was thus defined, subdivided into an n-dimensional grid (usually consisting of 50 or 100 logarithmically spaced R_i values), and used to calculate a $\{G(R_i,\tau)\}_{1\le i\le n}$ set of matrix exponents. The NNLS routine provided by the Matlab 6.2 software package (The MathWorks Inc.) was then used to search, for each ν value, the n-th dimensional $A_i = A_\nu(R_i)$ vector that minimized the deviation

$$\sigma^2 = \sum_\tau [P(\nu,\tau) - \sum_{i=1}^{n} A_i G(R_i,\tau)] \qquad (4)$$

The amplitude vectors leading to the smallest σ deviations for each particular ν value were then assembled in a row-by-row fashion to construct the complete 2D $I(\nu,R)$ RAS spectrum. The accuracy of this multiexponential fitting is actually dependent on the manner the experimental τ-values are chosen. In the present study, these times were sampled according to the logarithmic recipe $\tau_j = \tau_{\min}2^{(j-1)/M}$, where $M = (N-1)\ln(2)/\ln(\tau_{\max}/\tau_{\min})$ depends on the total number of recovery times $\{\tau_j\}_{1\le j\le N}$ employed, as well as on the minimum and maximum

(24) Callaghan, P. T. *Principles of Nuclear Magnetic Resonance Microscopy*; Oxford University Press: Oxford, 1991.
(25) Vlaardingerbroek, M. T.; Boer, J. A. D. *Magnetic Resonance Imaging: Theory and Practice*; Springer-Verlag: Berlin, 1999.
(26) Stilbs, P. *Prog. NMR Spectrosc.* **1981**, *19*, 1.
(27) Morris, K. F.; Johnson, C. S. *J. Am. Chem. Soc.* **1992**, *114*, 3139.
(28) Johnson, C. S. *Prog. NMR Spectrosc.* **1999**, *34*, 203.
(29) Antalek, B. *Concepts Magn. Reson.* **2002**, *14*, 225.
(30) Lee, J.-H.; Labadie, C.; Springer, C. S.; Harbison, G. S. *J. Am. Chem. Soc.* **1993**, *115*, 7761.
(31) Zumbulyadis, N.; Antalek, B.; Windig, W.; Scaringe, R. P.; Lanzafame, A. M.; Blanton, T.; Helber, M. *J. Am. Chem. Soc.* **1999**, *121*, 11554.
(32) Provencher, S. W. *Comput. Phys. Commun.* **1982**, *27*, 229.
(33) Morris, K. F.; Johnson, C. S. *J. Am. Chem. Soc.* **1993**, *115*, 4291.
(34) Antalek, B.; Windig, W. *J. Am. Chem. Soc.* **1996**, *118*, 10331.
(35) Delsuc, M. A.; Malliavin, T. E. *Anal. Chem.* **1998**, *70*, 2146.
(36) Stilbs, P. *J. Magn. Reson.* **1998**, *241*, 236.

recovery times τ_{min}, τ_{max}.[37] We also found it convenient to define this interval by following the literature suggestion $\tau_{min} \approx 0.2/R_{max}$, $\tau_{max} \approx 5/R_{min}$; R_{min} and R_{max} being the rates of the slowest and fastest relaxing sites in the sample.

The algorithm of the preceding paragraph was tested on a variety of model compounds using ^{23}Na (a 100% natural abundance spin−3/2 with 9×10^{-2} receptivity), ^{35}Cl (a 76% natural abundance spin−3/2 with 3×10^{-3} receptivity) and ^{25}Mg (a 10% natural abundance spin −5/2 with 2×10^{-4} receptivity, monitored after enrichment to 90%) as targets of investigation. Static and spinning experiments were recorded either at 7.1 T using a laboratory-built console equipped with a widebore Magnex magnet, or at 14.1 T using a Varian/CMX InfinityPlus console equipped with a widebore Oxford magnet. In all cases, 4 mm double-resonance Varian/CMX MAS probeheads were used. These experiments focused on central $-1/2 \leftrightarrow +1/2$ transitions and involved fitting saturation-recovery data, even if preliminary calculations revealed that fits would have had greater accuracy upon inputting inversion−recovery data. This was done due to the difficulty in achieving a homogeneous inversion of the central transition quadrupole line shapes, affected as they were by orientation-dependent nutation effects.[8,9] Data collection along the direct domain was carried out using a either single π-pulse or a train of π-pulse echoes; further details are described below. Preliminary proton relaxation measurements discriminating sites according to their distinctive rotating-frame decay rates were also assayed, as is also described below.

Results

We begin by discussing 2D RAS NMR results obtained on systems made by mixing simple single-site compounds whose individual line shapes could be a priori characterized. Figure 1 illustrates ^{23}Na NMR results observed on a powdered sample made up from a 50% w/w mixture of sodium sulfate and sodium carbonate. The static spin−echo line shape arising from this mixture at 7.1 T consists of a single featureless peak (Figure 1A), broadened by a combination of homonuclear dipolar couplings and second-order quadrupole effects. Yet a 2D RAS approach finds no difficulties in separating the two sites contributing to this static line shape (Figure 1B), even if the sites' apparent relaxation parameters are not extremely different. An interesting feature illustrated by this 2D spectrum is a slight dependence of the apparent relaxation rate observed for each of the sites, on the resonance frequency within the powder pattern. This behavior is suggestive of an anisotropy in the spin relaxation which, though only a minor complication toward achieving resolution for this particular sample, could complicate 2D RAS experiments on other systems. Yet the fact that the apparent frequency dependence appears correlated for the two sites in the mixture, lead us to believe that its origin is numerical and not physical. Indeed as we further detail below, common experimental artifacts may result in such systematic curving of the data upon using the NNLS processing routine. To deal with such effects a simple post-NNLS numerical procedure was developed, that accounted for this artifact by computing the various relaxivity values contributing to each particular frequency and assigning them to the average relaxation rate of each site (Figure 1C). In essence, no serious complication that could be unambiguously ascribed to relaxation anisotropy was observed in the various samples investigated during the course of this study.

Multisite samples involving nuclei with good receptivity such as ^{23}Na can be analyzed appropriately using single spin−echo

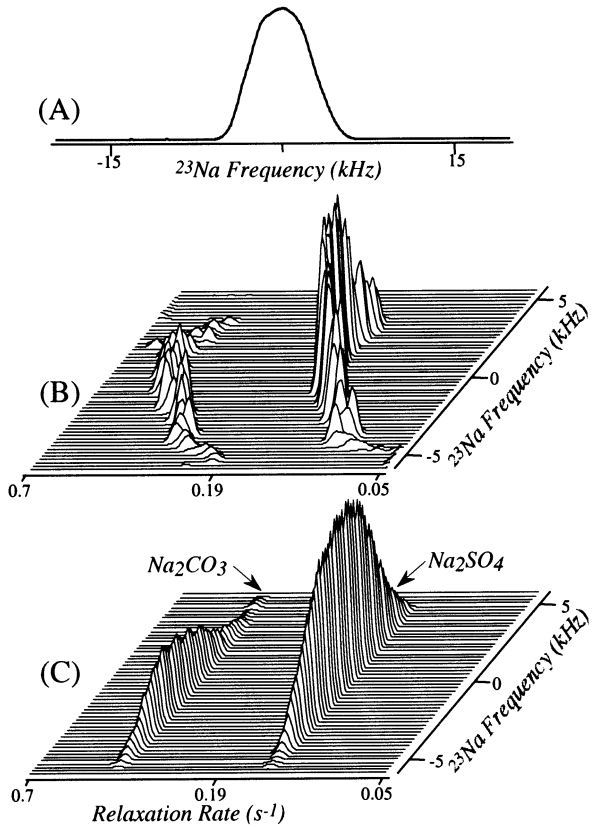

Figure 1. Comparison between the conventional (A) and 2D RAS NMR spectra (B) arising from a 1/1 mixture of Na_2SO_4/Na_2CO_3 powders. All data were recorded on a static sample at 14.1 T (158.7 MHz Larmor frequency). The RAS spectrum arose from a saturation-recovery experiment employing 20 τ recovery times logarithmically spaced between 0.04 and 40 s, with 64 scans recorded for each τ value. As for all experimental data sets described in this work, 100 logarithmically spaced relaxation rates R were used in the NNLS fitting of the recovery data. For the 256 frequency-domain points usually involved in the experiments, such procedures then demanded 30′ of processing time on a 2 GHz Pentium IV-based PC. The similar curvatures that the two RAS-resolved line shapes show in the (ν,R)-plane are suggestive of a common artifact, which could be compensated by placing the skyline projections of the individual powder patterns at the average relaxation rate exhibited by each site (C).

experiments. When focusing on lower-γ nuclei, however, gains have been shown from the implementation of CPMG on the quadrupole's central transition.[21−23] Since facilitating high-resolution studies that rely on this approach is one of the main forces driving the present study, we explore next the application of such strategy to ^{35}Cl NMR, a moderately insensitive spin probe. The large quadrupole moment and small magnetogyric ratio of this chlorine isotope (the most sensitive of the ^{35}Cl/^{37}Cl pair) implies that a considerable second-order quadrupole broadening may occur even when dealing with fairly symmetric electronic environments. Such was indeed the situation encountered upon exploring the line shapes arising from amino acid and peptide hydrochlorides;[38,39] ornithine and lysine hydrochloride powders, for instance, originate central transition line widths of ≈50 kHz even at the intense field used here for their study (14.1 T). Such large line widths would make their peak separation impractical by most spinning-based methodologies currently available. By contrast, resolution of these sites is

(37) Hinton, D. P.; Johnson, C. S. *J. Phys. Chem.* **1993**, *97*, 9064.

(38) Bryce, D. L.; Gee, M.; Wasylishen, R. E. *J. Phys. Chem. A* **2001**, *105*, 10413.

(39) Medek, A.; Frydman, L. Unpublished results.

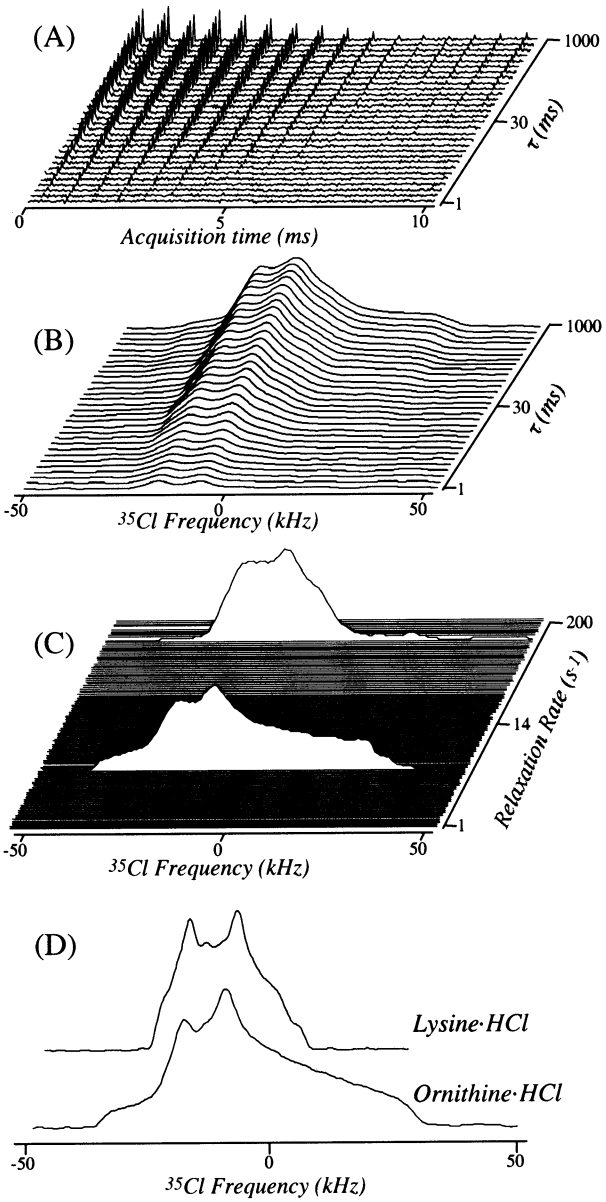

Figure 2. Processing stages involved in the relaxation-based separation of the overlapping second-order quadrupolar patterns arising from a 1/1 L-ornithine/L-lysine hydrochloride mixture, analyzed as a static powder at 14.1 T (58.8 MHz ^{35}Cl Larmor frequency). (A) ^{35}Cl CPMG echo trains recorded during the course of a saturation-recovery experiment involving 30 τ values logarithmically spaced between 1 and 1000 ms, with 1024 scans collected for each of these recovery times. (B) Saturation-recovery profile of the ^{35}Cl powder line shape resulting from the separation, Fourier processing and recombination of the individual CPMG echoes. (C) Averaged 2D RAS spectrum arising from the NNLS processing of the saturation-recovery data, separating the lysine powder pattern from its ornithine counterpart. For further comparison the spectra in (D) illustrate the static, ^{1}H-decoupled powder line shapes that could be observed for the individual amino acids under similar experimental conditions.

straightforward after only a few hours of data acquisition using the RAS-based strategy. Figure 2 summarizes selected processing stages involved in such a T_1-based analysis. These begin with the acquisition of several CPMG free-induction decays as a function of the recovery time τ that follows an initial saturation sequence (Figure 2A). This experimental data set is then processed by separating the various echo signals, adding them up for each individual τ value, weighting, zero-filling, and Fourier processing them. All this originates a quality saturation-recovery series of powder patterns ready to be fitted (Figure 2B). NNLS analysis of the individual frequency points within these line shapes followed by the averaging correction mentioned in the preceding paragraph yields clearly resolved powder patterns (Figure 2C), for the otherwise seriously overlapping resonances of the two salts. The powder patterns that can be resolved in such manner can be successfully compared with the second-order static patterns arising from the individual components of this mixture (Figure 2D), thus suggesting 2D RAS as a useful alternative not only for the separation but also for the spectroscopic characterization of different sites.

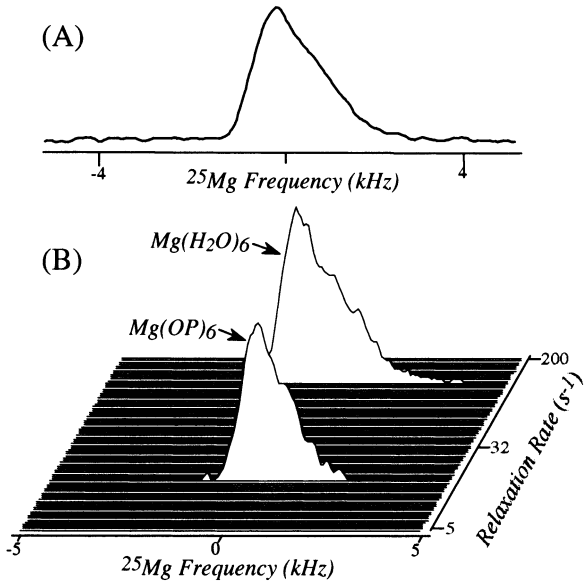

Figure 3. Comparison between conventional (A) and 2D RAS NMR spectra (B) acquired for MgATP/BPA at 14.1 T. Data were recorded at a 36.6 MHz Larmor frequency utilizing MAS at 10.0 kHz, a 10 kHz spectral width, and ^{1}H decoupling during the acquisition. The RAS spectrum arises from a saturation-recovery experiment employing 18 τ recovery times, logarithmically spaced between 2 and 500 ms (256 transients recorded for each τ). An averaging procedure following the NNLS fit of the data lead was also used in this case.

The potential of this new approach was also explored toward the characterization of the ternary magnesium(II), adenosine-5′-triphosphate, bis(2-pyridylamino) (for short, MgATP/BPA) nucleotidic complex. This sample possesses two distinct metal coordination environments in its unit cell: one where the Mg is octahedrally coordinated to six oxygen atoms coming from phosphates groups in inequivalent ATP molecules, and another where the Mg is octahedrally bound to six oxygens coming from waters of hydration.[40] These two sites give origin to overlapping central transition powder patterns, which though not resolvable by MAS (Figure 3A) can be separated by MQMAS NMR acquisitions. The different coordination environments of the two Mg sites, coupled to the importance that the relatively mobile waters of hydration usually have in determining spin−lattice relaxation in crystalline solids, make out of this complex a suitable candidate for testing the RAS protocol. A static experiment was thus assayed on a suitably crystallized sample where the complex's magnesium sites had been enriched to ≈90%. Although considerably strong signals were obtained from such system using a static CPMG sequence in combination with ^{1}H decoupling, problems arose from the relatively intense signals

(40) Cini, R.; Burla, M. C.; Nunzi, A.; Polidori, G. P.; Zanazzi, P. F. *J. Chem. Soc., Dalton Trans.* **1984**, 2467.

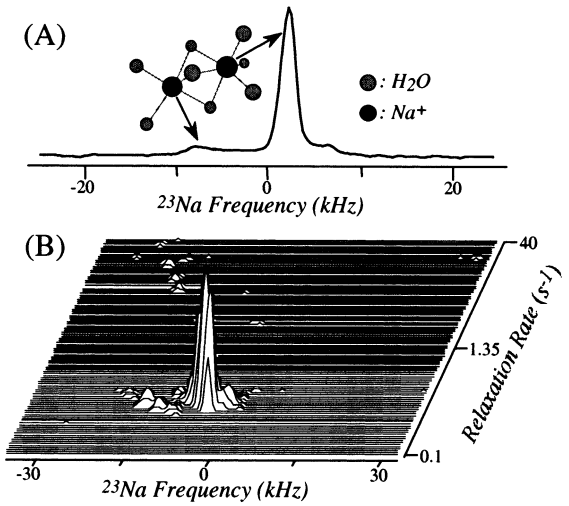

Figure 4. Comparison between conventional (A) and 2D RAS (B) ^{23}Na NMR spectra collected for Na_2dCMP(5′)·$7H_2O$ at 7.2 T (79.9 MHz Larmor frequency). Acquisition of the RAS data was made on a static powdered sample using a laboratory-built NMR spectrometer and the following conditions: 70 kHz spectral width, ^{1}H decoupling during the acquisition, 22 τ recovery times logarithmically spaced between 0.025 and 25 s, and 700 scans for each τ. For the sake of clarity, this stack plot is shown without implementing the averaging procedure that follows the NNLS processing.

emerging in this case from the magnesium forming part on the probehead's unenriched background. Background signals were by contrast negligible upon analyzing the nucleotide under MAS, which was therefore incorporated into the measurements. Figure 3B illustrates the 2D RAS separation that could then be achieved for the two sites in the nucleotide. Though the powder line shapes arising from such separation were not as featured as those in the ^{35}Cl analysis, sites could still be clearly resolved within a fraction of the time it took us to setup and collect an analogous MQMAS-type experiment. Furthermore, this 2D RAS result indicates that the site with largest quadrupole coupling of the pair is also the one characterized by the faster T_1 relaxation; since it is reasonable to expect such fast-relaxing site to be the one coordinated by the six water molecules, this corroborates the assignment previously made on the basis of the MQMAS and ^{1}H−^{25}Mg REDOR experiments.[41]

Though clearly useful in the cases described so far, instances arise where the relaxation-based separation of powder patterns is unsuitable. Indeed, just as sites with similar chemical environments may not be resolvable according to their chemical shift differences, sites with similar relaxation environments will not be distinguishable by their relaxometry characteristics. The two inequivalent sodium sites within the unit cell of Na_2dCMP(5′)·$7H_2O$ furnish an example of such limitations. The ^{23}Na quadrupole coupling constants of the two sites in this deoxycytosine salt are considerably different, as one of these resides in a highly asymmetric pentacoordinated environment while the other one sits in a hexacoordinated, symmetric one.[42] Yet both sodium sites partake of the same water-capped, water-bridged dimer structure, a feature which endows them with similar chemical shifts and, presumably, with nearly identical spin−lattice relaxation times. Thus, whereas two very distinct second-order quadrupolar line shapes can be appreciated in the

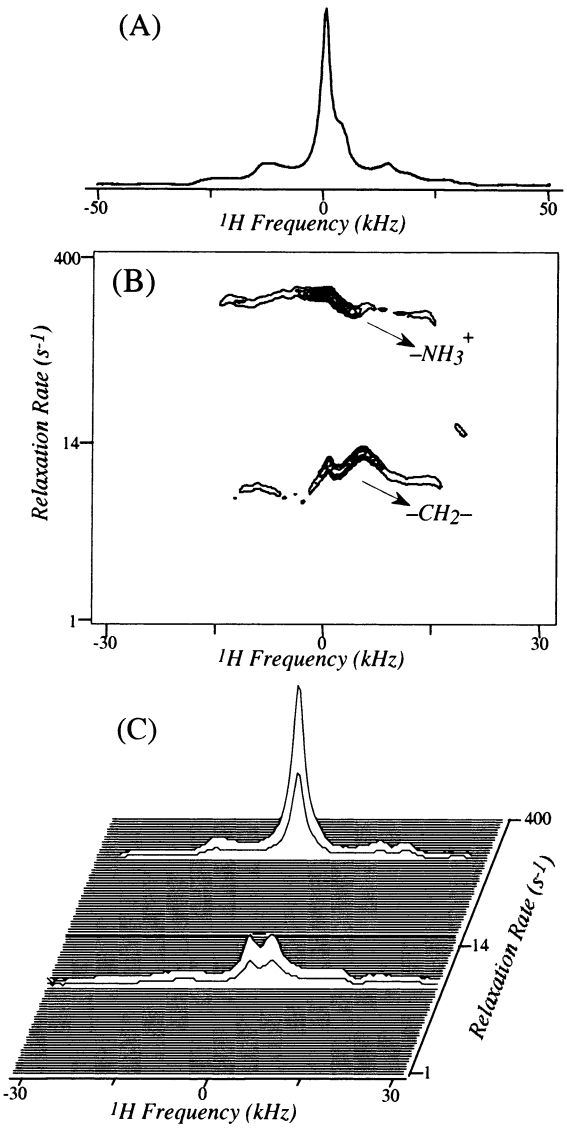

Figure 5. Exploitation of $T_{1\rho}$ relaxation rate differences in the Lee−Goldburg frame, toward the resolution of inequivalent ^{1}H sites in a powdered solid. (A) 14.1 T NMR spectrum recorded for a glycine sample at a MAS rate of 14.0 kHz: spinning sidebands are visible in this spin−echo experiment (echo time = 71.4 μs), but chemical sites are barely resolved. (B) 2D RAS spectrum arising from a data set collected under similar conditions, upon monitoring the ^{1}H magnetization remaining after a spin-lock delay along the magic-axis. Eighteen τ decay times logarithmically spaced between 0.5 and 100 ms were used in the NNLS reconstruction leading to this contour plot, with 16 phase-cycled scans acquired for each of these τ values. The rate of spin nutation associated to the effective spin-locking field was 70 kHz. (C) Stack plot arising upon subjecting the data set in (B) to the averaging procedure described for the quadrupolar cases.

nucleotide's static ^{23}Na spin−echo spectrum, nearly no additional resolution is afforded by a 2D ^{23}Na RAS procedure based on T_1 discrimination (Figure 4). Also interesting to remark is the minor cross-talk arising in this 2D spectrum between the real peaks and regions of higher relaxivity values, artifacts which we believe are a consequence of the small relative intensity that for each frequency point is displayed by the pentacoordinated site.

We conclude this experimental account by exploring the application of 2D RAS-based algorithms to the study of another type of spin system where achieving site resolution is often problematic. The case in question involves solid-state proton

(41) Grant, C. V.; Frydman, V.; Frydman, L. *J. Am. Chem. Soc* **2000**, *122*, 11743.
(42) Pandit, J.; Seshadri, T. P.; Viswamitra, M. A. *Acta Crystallogr.* **1983**, *C39*, 342.

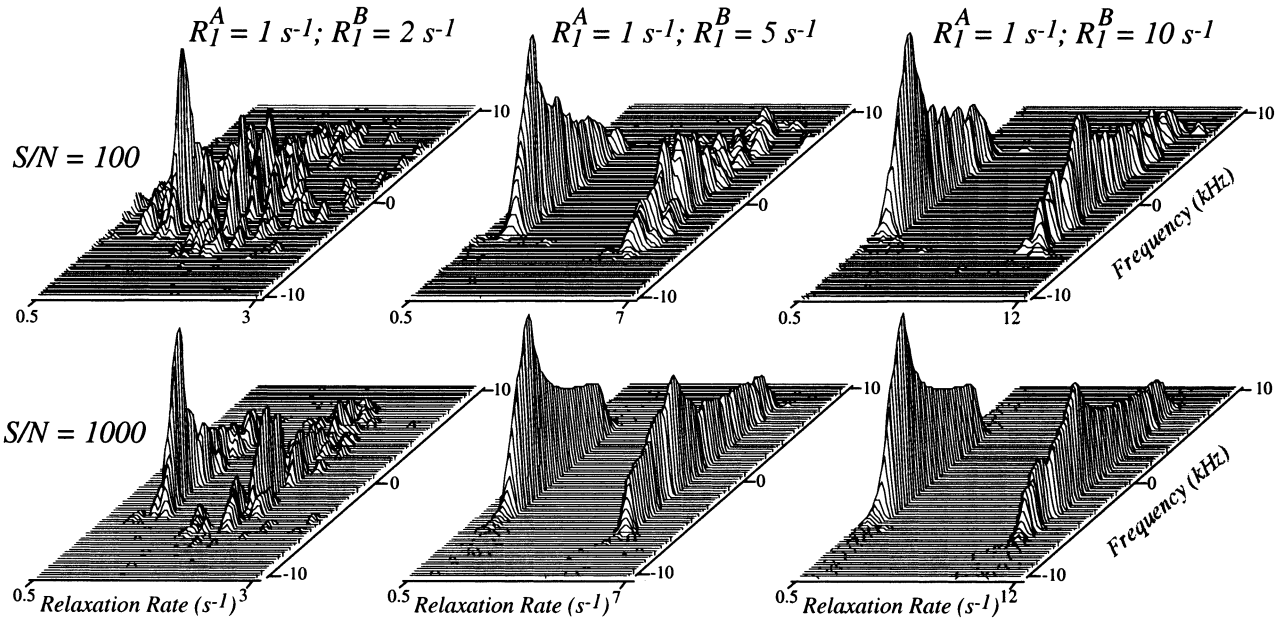

Figure 6. Resolving characteristics of the NNLS fitting procedure, as viewed for different values of the S/N ratio affecting the input relaxation data. All 2D RAS sets were calculated for two equally populated sites possessing different chemical shielding anisotropies (span ≈ 8 kHz for site A, 13 kHz for site B), and the indicated longitudinal R_1 relaxation rates. The fitting was done assuming 50 logarithmically spaced R values, using as input ideal saturation-recovery data sets (30 points) to which white noise had been added.

NMR, where peaks arising from inequivalent sites are often broadened by an extensive network of dipole−dipole interactions. Fast MAS will narrow these dipole-broadened resonances,[5,6,43,44] yet given the currently achievable rates of sample spinning, resolving peaks arising from inequivalent sites still requires the application of additional multiple-pulse sequences.[3−6,43−45] Relaxation times might again be invoked to resolve overlapping resonances in this case, with the added advantage that the data fits will benefit from the superior S/N that is usual in proton spectroscopy. The extensive network of homonuclear interactions present in conventional organic/biological solids will actually tend to homogenize the T_1 and T_2 times of individual proton sites, thus making the kind of measurements that were described on quadrupoles nonspecific. On the other hand, relaxation times monitored within an interaction-frame that is inclined at the magic-angle with respect to the spins' z quantization axis will enjoy from a considerable decoupling among neighboring sites, giving the method a chance to achieve resolution among these. A simple option to achieve a separation based on the relaxation characteristics of individual chemical sites is thus offered by measuring $T_{1\rho}$ under so-called Lee−Goldburg conditions.[46,47] Figure 5 illustrates results obtained on the basis of this premise; it compares the standard single-pulse ^{1}H MAS trace obtained on a powdered glycine sample, against uncorrected and averaged 2D RAS spectra reconstructed from this relaxation process. As can be appreciated from these results the very different mobility characterizing groups in this molecule lead to $-CH_2-$ $T_{1\rho}$ times ca. an order of magnitude longer than those of the $-NH_3^+$, providing relaxation measurements with a simple route to separate the sites' resonances. Chemical differences are also reflected along the frequency axes of the now resolved MAS line shapes, with the center-of-mass of the amino peak appearing ca. 5 ppm higher than that of the methylene. Further examples on the application of this strategy, which though relying solely on moderate MAS rates avoids multiple-pulse sequences altogether, will be discussed elsewhere.

Discussion

The results presented in the previous section indicate that relaxation-based measurements constitute a promising alternative toward the resolution of inequivalent sites in solids. Simultaneously, however, these results open up a number of questions regarding the generality of the method. Most important among these are (i) how different need relaxation parameters be to allow for a successful RAS-based analysis, (ii) how sensitive is the method to instrumental instabilities, and (iii) how many overlapping powder patterns can the method resolve. These are actually complex issues, interdependent on one another: instrumental instabilities may compromise the number of sites that can be resolved, numerous sites may only become amenable to separation provided that their relaxation parameters are considerably different, etc. Furthermore, it is evident that an accurate, quantitative answer to these queries will also be highly dependent on the method that is employed for the numerical analysis of the data, among which the Matlab-based NNLS routine that was assayed in this study ranks probably as most basic. Yet it is perhaps because of its lack of sophistication, that it is worth exploring the conservative assessments arising when using this processing routine. We therefore decided to evaluate the approach's potential by focusing on a number of synthetic data sets, where the apparent relaxivity, number of sites, and kinds of artifacts involved could be easily manipulated.

(43) Hafner, S.; Spiess, H. W. *Concepts Magn. Reson.* **1998**, *10*, 99.
(44) Ray, S.; Vinogradov, E.; Boender, G.-J.; Vega, S. *J. Magn. Reson.* **1998**, *135*, 418.
(45) Maciel, G. E.; Bronnimann, C. E.; Hawkins, B. L. In *Advances in Magnetic Resonance: The Waugh Symposium*; Warren, W. S., Ed.; Academic Press: San Diego, CA, 1990; Vol. 14; p 125.
(46) Lee, M.; Goldburg, W. I. *Phys. Rev.* **1965**, *140*, 1261.
(47) Haeberlen, U.; Waugh, J. S. *Phys. Rev.* **1969**, *185*, 420.

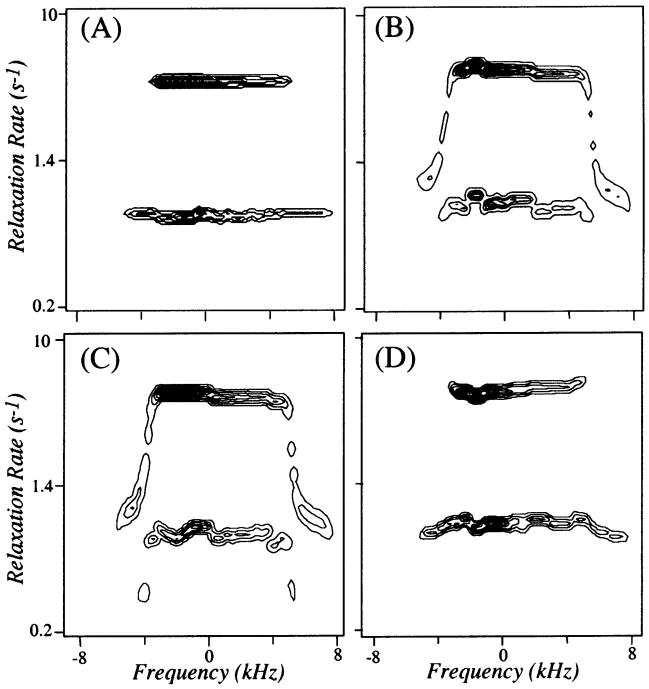

Figure 7. Effects introduced by frequency-domain baseline distortions on the NNLS fitting procedure, as viewed for two sites possessing simulation and processing parameters as in the center panel of Figure 6 (S/N = 1000, R_1's of 1 and 5 s^{-1} respectively). (A) Distortion-free benchmark. (B) Contour resulting after applying a DC baseline offset equal to +0.5% of the maximum signal intensity. (C) Same as B for a +0.5% DC offset superimposed on an additional baseline tilt of +0.5%. (D) Same as B for a −0.5% DC baseline offset. Notice the similarity between the edge distortions in panels B and C and those observed in experimental data sets (Figures 1B and 4B).

As an initial test, we explore the method's ability to resolve two inequivalent sites, when viewed as a function of the peaks' difference in relaxation rates and as a function of the overall quality of the data. For the sake of simplicity, two inequivalent sites affected by a static shielding anisotropy were assumed. From these tests it could be concluded that the relaxation rates between the sites to be resolved may differ by a factor of ≈2 when dealing with an excellent S/N (Figure 6), with a larger difference desirable for the kind of S/N characterizing our experimental acquisitions (S/N ≈ 100). Though short of ideal, and liable to degrade when dealing with sites with very unequal populations, this kind of resolution opens up a comfortable window for the analysis of a wide variety of solids. It should also be mentioned that an increase in noise immunity was also noted as the number of τ and R values incorporated into the fit were increased.

A second aspect that was explored meant to address the effects introduced on the 2D spectra by artifacts which are common in static solid-state NMR acquisitions. These included spectral distortions arising due to the spectrometer's deadtime, as well as common baseline artifacts such as DC offsets or tilts. 2D RAS simulations then predict that for a typical S/N of 100 dephasing effects will have no appreciable consequences, whereas baseline distortions may affect RAS fits even if relatively small. Among the changes that are then observed count some of the main artifacts detected during the course of our experiments (Figure 7), including a curvature of the spectral ridges from their ideal R values that becomes more noticeable toward the edges of the powder patterns, and which could easily be confounded with an anisotropy in the relaxation times.

A final aspect that we decided to probe was the method's separation performance when it comes to dealing with more than two sites. In this connection we observe that, although the NNLS algorithm can detect a high number of inequivalent sites within its range of R-fitting if given noiseless input data set, this ability degrades as S/N decreases. Figure 8 illustrates this feature with 2D RAS analyses of a model containing three inequivalent sites. It is to be noted, however, that some of these S/N limitations can be compensated by the incorporation of additional points into the relaxation data set being fitted. This characteristic will actually be highly sensitive on the method used for fitting the data; we thus defer a full analysis on the limits of the method until additional processing approaches are assayed.

Conclusions

The results described throughout the course of this work demonstrate the worthwhileness of exploring relaxation-based strategies, as they apply to the enhancement of resolution in solid state NMR. Among the main features of these strategies are the simplicity of the experiments they entail, the relatively short times associated with their setting up and data collection, and the ease with which resonances can be resolved in certain cases where no realistic alternatives exist for achieving this aim. Still, it is apparent that separating inequivalent sites via an inversion of the relaxation data into a new "spectral" dimension will only be feasible if a few basic conditions are met. One is that the relaxation parameters of the various sites that are to be characterized should be substantially different. Although this

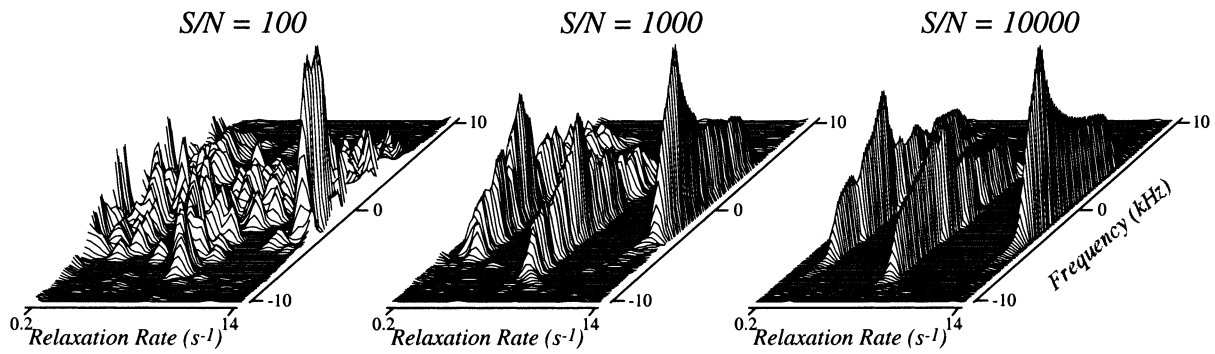

Figure 8. S/N dependence of results afforded by the NNLS analysis as applied toward the resolution of three inequivalent powder patterns. These were assumed to possess shielding spans of 13, 11, and 8 kHz, and relaxation rates of 1, 3, and 10 s^{-1} respectively (i.e., left-most panel in Figure 6, plus an additional site in the middle). Other simulation and fitting parameters were as in Figure 6.

is not always the case for a particular relaxation measurement, the possibility arises to introduce meaningful differences by switching observable (e.g., from T_1 to $T_{1\rho}$) or via changes in the sample's temperature. A second condition that needs to be met is the availability of high-quality data, a demand which is aided by the simple and efficient type of experiments that relaxation measurements usually involve. Finally, a successful implementation of 2D RAS NMR requires the availability of a robust data processing program. The kind of analysis carried out in the present study is in actuality fairly simple; intriguing therefore, is the possibility of assessing other, more sophisticated LT-type processing routines to improve the capabilities of the method. In fact, the incorporation of minor modifications into the DOSY processing routines that are nowadays available with most commercial NMR instrumentation would probably enable a much wider assessment and utilization of this kind of analysis. Given the promise carried by the incorporation of relaxation parameters into the tool kit available for improving resolution in solids NMR, such additional processing refinements appear likely.

Acknowledgment. We are grateful to Profs. M. Neeman (Weizmann Institute) and C. S. Johnson (University of North Carolina) for insight about non-Fourier processing methods and to Dr. V. Frydman (Weizmann Institute) for the enrichment and crystallization of the ATP sample. This work was supported by a Philip M. Klutznick Fund for Research (Weizmann Institute) and by the Israeli Science Foundation (Grant No. 296/01). A.L. is also grateful to the Feinberg Graduate School of The Weizmann Institute for an A. Stone fellowship.

JA021173M